Acta Cryst. (1977). A33, 706–712

Lattice Parameter Determination of Exsolution Structures in Labradorite Feldspars

BY A. OLSEN

Department of Physics, University of Oslo, Oslo, Norway

(*Received* 14 *December* 1976; *accepted* 3 *February* 1977)

Plagioclase feldspars with chemical formula $Na_{0.5}Ca_{0.5}Al_{1.5}Si_{2.5}O_8$ for their bulk composition consist of lamellar structures on the 1000 Å scale at low temperatures. The lamellae have different compositions as a result of exsolution. In electron-diffraction patterns certain of the Kikuchi lines from these lamellae are doubled. These have been utilized for lattice-parameter determination by a method which is based on measurements of the differences in the orientation of the atomic planes in the lamellae. The factors determining the accuracy are discussed. For two specimens it is found that there is a difference of about 0·005 Å between the *a* axes and about 0·15° between the γ angles in the two lamellae.

Introduction

Labradorite is the intermediate member of the plagioclase feldspars having the end members albite ($NaAlSi_3O_8$) and anorthite ($CaAl_2Si_2O_8$). The structures of these intermediate plagioclases have been a matter of controversy for nearly 25 years; for a summary see Smith (1974*a*,*b*). Recently, electron microscopy has made significant contributions to a clarification of the crystallography associated with these minerals (McLaren & Marshall, 1974; Hashimoto, Kumao, Endoh, Nissen, Ono & Watanabe, 1976; Hashimoto, Nissen, Ono, Kumao, Endoh & Woensdregt, 1976). Specimens in the composition range from about 42 to 58 mol % anorthite (An) (and mostly containing 2–4 mol % potassium feldspar) consist at low temperatures of lamellar and domain structures on three different scales. Firstly, the structure is a superlattice which is seen as fringes of 30–50 Å associated with the *e*-type and *f*-type satellites found in X-ray and electron-diffraction patterns. Secondly, there is a domain texture on the 200–500 Å scale which is particularly clear in dark-field micrographs (McLaren & Marshall, 1974; Hashimoto, Nissen, Ono, Kumao, Endoh & Woensdregt, 1976). Thirdly, one finds a lamellar structure on the 1000 Å scale which causes iridescence (or the Schiller effect). These lamellae have been said to result from the exsolution into two chemically different plagioclases; a direct analysis of their composition with transmission electron microscopes fitted with an X-ray analysis attachment confirms that the composition of the two lamellae differ in anorthite content, typically about 40 mol % An and 60 mol % An (Nissen, Champness, Cliff & Lorimer, 1973; Cliff, Champness, Nissen & Lorimer, 1976; Olsen, 1976*b*; Olsen & Lillebö, 1976).

Structural differences between the two sets of lamellae are very slight. The main spots in X-ray and electron-diffraction patterns indicate only one lattice, and hence it has not been possible to determine the lattice constants of the two members by X-ray diffraction. In the electron microscope the lamellae can easily be observed in bright and dark-field images. The contrast from them differs, thus indicating different orientations of the atomic planes. In the electron-diffraction patterns certain of the Kikuchi lines are doubled (Nissen & Bollmann, 1968) and recently Olsen & Lillebö (1976) reported a study of a labradorite where these doubled lines were utilized for the lattice-parameter determination. Two methods were applied. The first, the Kikuchi-line intersection method (Olsen, 1976*a*) which was an extension of the method by Høier (1969) to lower symmetry cases than cubic, could only detect differences in γ. The second, which is reported here, is referred to as the split-Kikuchi-line method and can be used to determine all the lattice parameters.

Determination of lattice parameters of slightly different phases is a general problem in crystallography. Since few details of the split-Kikuchi-line method were given in the earlier report (Olsen & Lillebö, 1976), the purpose of the present paper is to give a more complete description of the method as well as to report new lattice-constant determinations and to present a more detailed discussion of the accuracy attainable.

Theory

General description

Various methods for orientation determination of crystals from Kikuchi patterns have been described (Johari & Thomas, 1969; Pumphrey & Bowkett, 1970; Faivre, 1975). It has been shown that a misorientation of a few minutes of arc between two subgrains may be detected from the splitting of the lines in a selected-area diffraction pattern taken across the sub-boundary. In such cases the misorientation of the crystals can be described by a rotation about one axis.

In the present labradorite case, however, the two lamellae have different lattice parameters. Therefore, the misorientation across the lamellar boundary of different lattice planes has to be described by different rotation axes.

The split-Kikuchi-line method is based upon meas-

urements of the misorientation across boundaries between exsolution lamellae and consists of the following steps. (1) The misorientation (the angle φ) between the lattice planes in the two lamellae is measured from the Kikuchi patterns. (2) The orientation of the lamellar boundary is determined by trace analysis (Hirsch, Howie, Nicholson, Pashley & Whelan, 1965). (3) A model microstructure is assumed in which the boundary is an invariant plane so that the structure of the two lamellae is described as a result, for the mean structure, of the operation of shears parallel to the lamellar plane and expansions and contractions normal to this plane. From the different lattice parameters for the two phases theoretical φ values are calculated. (4) The experimental and theoretical φ values are compared in a stereographic projection based on the mean lattice constants.

Determination of the misorientation from the Kikuchi pattern

Let us assume that the misorientation φ of the lattice planes in the two lamellae can be described by a rotation about an axis lying in a plane parallel to the photographic plate. The splitting of the Kikuchi lines is then related to the angle φ by the following expression:

$$\varphi = \left(\frac{\Delta S}{2R}\right)\left(\frac{\lambda}{d}\right) \tag{1}$$

where ΔS is the distance measured on a photographic plate between the split lines, $2R$ the distance between the excess and the defect line and d the mean plane distance. λ is the wavelength of the electrons and can be determined from Si standards by the Kikuchi-line intersection method (Høier, 1969; Olsen, 1976*a*). (1) is an approximate relation, based on the assumption of small scattering angles and small misorientations, and follows immediately from Bragg's law and the geometry of the Kikuchi pattern. In practice, these approximations do not limit the accuracy of the orientation determinations. The main problem is associated with the determination of the axis which describes the relative orientation of the lattice planes in the two lamellae. The magnitude of the splitting of a particular Kikuchi line depends on the orientation of this rotation axis and is maximum when this axis is normal to the incident electron beam. Therefore, a number of measurements of the splitting of a particular line have to be made in different projections in order to determine the maximum value.

The structure model

The model of the microstructure is based on theories for crystalline interfaces (Bollmann, 1970).

Let **a**, **b**, **c** be the basic vectors of the triclinic mean structure. This triclinic lattice is then described in an orthogonal coordinate system where the z axis is perpendicular to the boundary plane between the two lamellae and the x and y axes are parallel to this plane. The y axis lies along the intersection between the **a*****c*** plane and the lamellar plane. Shears along the x axis and the y axis and an expansion (or contraction) along the z axis are now applied to the mean lattice in order to transform it into the lattices of the two lamellae. The triclinic lattice constants of the two lamellae can then be found.

This procedure can be expressed by the following: We introduce the cell matrix

$$\mathbf{u}_0^* = \begin{pmatrix} \mathbf{a}^* \\ \mathbf{b}^* \\ \mathbf{c}^* \end{pmatrix} \tag{2}$$

with the reciprocal basis vectors of the mean structure as its elements. The transformation from this mean lattice to the lattice of lamella No. 1 can therefore be written:

$$\mathbf{u}_1^* = \mathbf{Q}^{-1}\mathbf{D}_1\mathbf{S}_1\mathbf{Q}\mathbf{u}_0^* = \mathbf{A}_1\mathbf{u}_0^* \tag{3}$$

where $\mathbf{u}_1^*$ is the cell matrix for lamella No. 1 in analogy with (2). $\mathbf{D}_1$ and $\mathbf{S}_1$ describe the deformation and the shears which must be applied to the mean lattice and are given by

$$\mathbf{D}_1 = \begin{pmatrix} 1 & 0 & 0 \\ 0 & 1 & 0 \\ 0 & 0 & 1+\varepsilon_1 \end{pmatrix}, \tag{4}$$

$$\mathbf{S}_1 = \begin{pmatrix} 1 & 0 & \tan\sigma_{1x} \\ 0 & 1 & \tan\sigma_{1y} \\ 0 & 0 & 1 \end{pmatrix}. \tag{5}$$

The matrix $\mathbf{Q}$ (with its inverse $\mathbf{Q}^{-1}$) describes the coordinate transformation from a triclinic to an orthogonal coordinate system and is expressed by:

$$\mathbf{Q} = \begin{pmatrix} l_1 & m_1 & n_1 \\ l_2 & m_2 & n_2 \\ l_3 & m_3 & n_3 \end{pmatrix} \tag{6}$$

where

$$\begin{aligned} l_1 &= \frac{M^2 ab\cos\gamma - pq}{M\sqrt{(M^2b^2-q^2)}}, & m_1 &= \frac{b^2M^2-q^2}{M\sqrt{(M^2b^2-q^2)}}, & n_1 &= \frac{M^2bc\cos\alpha - qr}{M\sqrt{(M^2b^2-q^2)}}, \\ l_2 &= -\frac{qS_{23}+rS_{33}+pS_{31}}{V\sqrt{(M^2b^2-q^2)}}, & m_2 &= 0, & n_2 &= \frac{qS_{12}+rS_{13}+pS_{11}}{V\sqrt{(M^2b^2-q^2)}}, \\ l_3 &= \frac{p}{M}, & m_3 &= \frac{q}{M}, & n_3 &= \frac{r}{M}. \end{aligned} \tag{7}$$

$M=1/d_{pqr}$ where d_{pqr} is the distance between the (pqr) planes. V is the volume of the unit cell of the mean lattice and $S_{ij}(i,j=1,2,3)$ have their usual crystallographic meanings (Appendix). (pqr) is the boundary plane between the two lamellae.

For lattice 2 the cell matrix is obtained as in (3):

$$\mathbf{u}_2^* = \mathbf{Q}^{-1}\mathbf{D}_2\mathbf{S}_2\mathbf{Q}\mathbf{u}_0^* = \mathbf{A}_2\mathbf{u}_0^* . \quad (8)$$

The relation between the basic vectors in reciprocal and real space for the mean lattice can be written:

$$\mathbf{u}_0^* = \mathbf{T}_0\mathbf{u}_0 \quad (9)$$

where

$$\mathbf{T}_0 = \frac{1}{V^2}\begin{pmatrix} S_{11} & S_{12} & S_{13} \\ S_{12} & S_{22} & S_{23} \\ S_{13} & S_{23} & S_{33} \end{pmatrix}. \quad (10)$$

Similar relations hold for lattices 1 and 2. Hence:

$$\mathbf{u}_1^* = \mathbf{A}_1\mathbf{A}_2^{-1}\mathbf{T}_2\mathbf{u}_2 = \mathbf{U}\mathbf{u}_2 . \quad (11)$$

The angle between the lattice planes (hkl) in lattices 1 and 2 can now be calculated. The relation (11) will simplify these calculations since $\mathbf{u}_1^*$ is expressed in terms of $\mathbf{u}_2$.

For a given orientation of the boundary between the lamellae, the six parameters σ_{1x}, σ_{1y}, ε_1 and σ_{2x}, σ_{2y}, ε_2 can be varied and the angles φ for the different lattice planes calculated. The best fit between the observed and the calculated φ values determines the lattice parameters for the two phases.

Experimental

Three specimens with compositions near 50 mol % An have been studied. Lattice parameters for one of the specimens (from Labrador) have been reported previously by Olsen & Lillebö (1976). In that paper it was suggested that the accuracy of the lattice-constant determination by the split-Kikuchi-line method depends mainly on the accuracy of the mean lattice constants determined by X-ray diffraction. In order to get better accuracy this specimen has been studied further by X-ray diffraction and more accurate results for this specimen will be reported here. One of the other investigated specimens showed no iridescence, no exsolution lamellae in the electron microscope and no split Kikuchi lines, but is included in the present study for comparison purposes.

Thin sections parallel to (010) and (001) were ion-thinned and studied at 80 and 100 kV in a Philips EM 300 microscope equipped with an EDAX energy dispersive X-ray analyser. Some dark-field images were also taken at 200 kV in a JEM 200A microscope.

Details of the specimens are given in Table 1. In the text they will be referred to as *L*, *A*, *A*1. The mean composition of the specimens was determined by electron microprobe analysis.

Table 1. *Details of specimens examined*

Specimen	Locality	Mean composition (mol %) An	Ab	Or	Optical feature
L	Labrador, Canada	53·4	44·9	1·7	Iridescence
A	Åna-Sira, Norway	50·6	46·6	2·8	Iridescence
*A*1	Åna-Sira, Norway	47·9	47·1	5·0	No iridescence

X-ray powder diffraction photographs were taken with a Guinier camera with monochromatized Cu $K\alpha_1$ radiation ($\lambda=1{\cdot}54051$ Å) and with Si used as internal standard. The mean lattice parameters were then obtained by a least-squares refinement of the diffraction data. In order to take into account variations in the mean composition and the lattice constants, two powder patterns were recorded from each specimen.

Transmission electron microscopy

Domain structures

The two specimens *L* and *A* were found to be very similar. Both consist of alternating lamellae with a periodicity about 1600–2000 Å which produce iridescence. The orientation of the lamellar boundaries was determined by trace analysis and found to lie near $(\bar{4},24,3)$ (referred to the albite unit cell) in both cases. The composition of these lamellae has been studied previously and is about 40 and 60 mol % An (Olsen, 1976*b*; Olsen & Lillebö, 1976). The *e* and *f*-type satellite reflexions were present in diffraction patterns from both specimens and correspond in both cases to a superstructure with a periodicity about 32 Å in the $[112]^*$ direction in reciprocal space (again referred to the albite unit cell). As discussed by Hashimoto, Nissen, Ono, Kumao, Endoh & Woensdregt (1976), the spacing of the *e* and *f* fringes cannot be used as a measure of the composition of the minor and major Schiller lamellae, but may be a function of the bulk anorthite composition (Bown & Gay, 1958). From the diagram given by Smith (1974*a*) of the wavelength of the superstructure as a function of the bulk anorthite content, the observed *e* spacings correspond to a mean composition of (52 ± 2) mol % An.

Dark-field microscopy using a pair of the *e*-type satellite reflexions from specimen *A* revealed the domain structures shown in Fig. 1. A random distribution of domains (200–500 Å in size) was observed. This irregular domain structure is similar to the structure observed by McLaren & Marshall (1974) in An_{32}.

Kikuchi patterns

In the electron diffraction patterns certain of the Kikuchi lines were doubled. The patterns from the specimens *L* and *A* were very similar (Fig. 2). In some projections no doubled lines were observed (Fig. 2*a*). Some of the lines are very sharp and some broad and

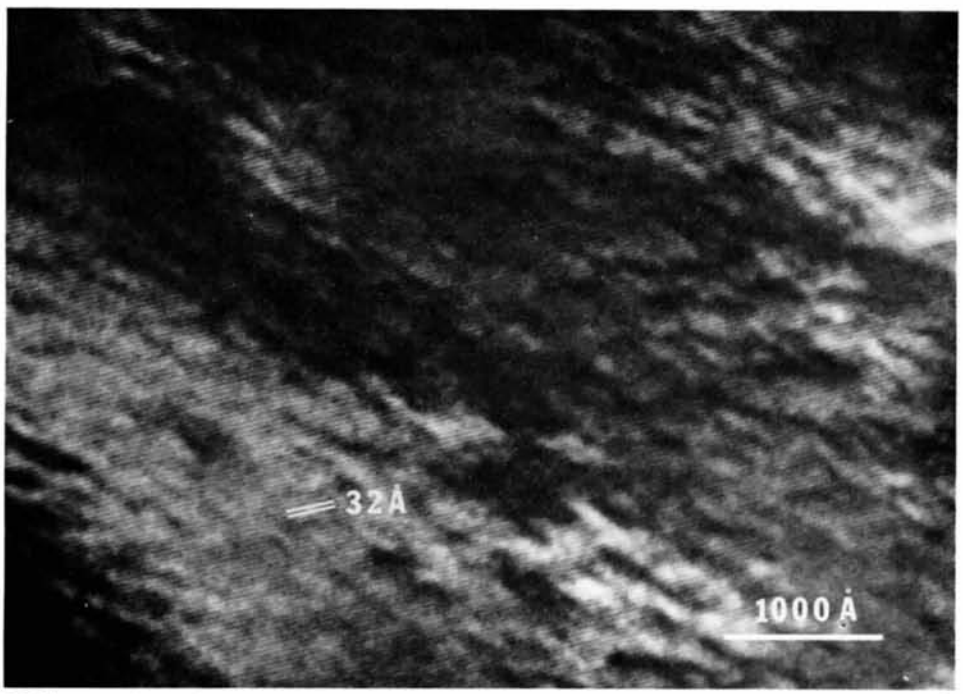

Fig. 1. Dark-field image of specimen *A* using a pair of *e* reflexions. The lamellae (periodicity about 2000 Å), a domain texture (200-500 Å) and the superlattice (32 Å) can be recognized. 200 kV.

[*To face p.* 708

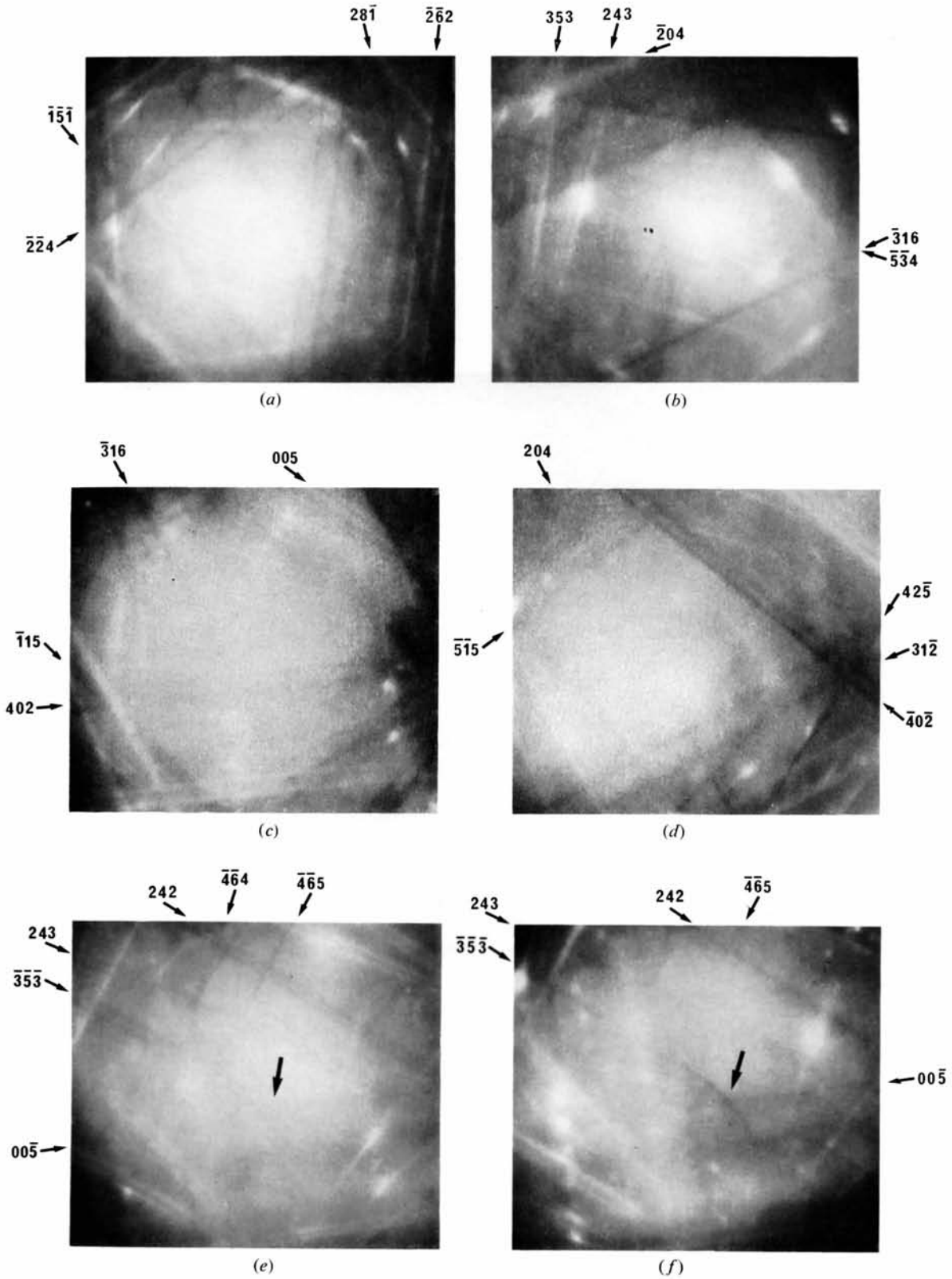

Fig. 2. Kikuchi patterns from the specimens *L* (left) and *A* (right).

diffuse. The maximum splitting was found to occur for both specimens for the lines 402 [Fig. 2(*c*) and (*d*)]. The similarity between the Kikuchi patterns from the two specimens is well demonstrated in Fig. 2(*e*) and (*f*). The superstructure (~32 Å) or the domain structure (~200–500 Å) do not give rise to the doubled Kikuchi lines. These lines are due to the lamellae (~1000 Å) which have different compositions.

The intensity ratio of the two split lines was nearly constant across specimen *L*, but varied in specimen *A*, whereas the distance between the lines changed only slightly. This indicates the composition and lattice constants of the two exsolved phases to be similar across the specimen, whereas the volume fraction of the two phases (and hence mean composition) varies.

The procedure for indexing the Kikuchi lines was greatly simplified by computer generation of Kikuchi patterns. The applied method was similar to the procedure developed by Pirouz & Boswarva (1974).

The separation was measured for about 85 Kikuchi lines from *L* and 93 lines from *A*. The angles φ were calculated and the maximum values for each line plotted in stereographic projections based on the mean lattice constants (Fig. 3). φ values less than 0·1° are not given because of the low accuracy in these measurements. The diameter of the experimental points (the filled circles) is proportional to the value of φ.

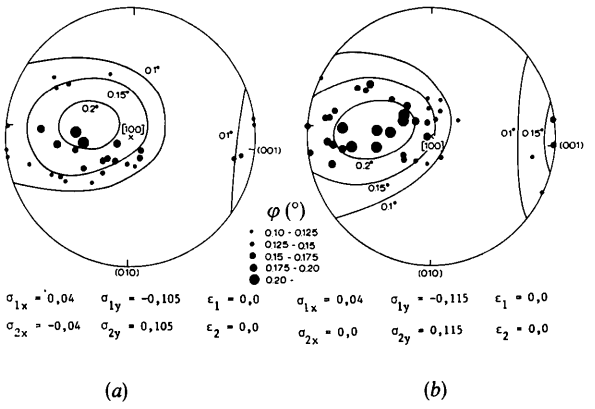

(*a*) (*b*)

Fig. 3. The angle φ plotted in a stereographic projection for specimens *L* (*a*) and *A* (*b*). The diameter of the experimental points (the filled circles) is proportional to the value φ. Theoretical values (the curves) with lattice parameters for the best fit (see Table 2) are indicated. Invariant plane: $(\bar{4},24,3)$.

A number of shear and expansion (or contraction) parameters were tried in order to reproduce the observed φ values. The results for the best agreement with the experimental points are shown in Fig. 3.

The lattice constants for all three specimens are given in Table 2. The indicated accuracies of the parameters are discussed in the next section.

Discussion

Accuracy of the method

Since the mean lattice constants are determined by X-ray diffraction from a different section of the crystal to that studied by electron diffraction, a careful selection of specimens is required. The accuracy in the determination of the lattice parameters by the split-Kikuchi-line method depends, then, mainly upon the accuracies in the following. (1) The shear and expansion (contraction) parameters. (2) The orientation of the lamellar boundaries. (3) The mean lattice constants. (4) The variations in the mean composition. (5) The determination of φ.

Points (3), (4), (5) have been discussed elsewhere in this paper.

The influence of the shear and expansion parameters was studied by varying them around the values which gave the best fit with the measurements. As may be seen from Fig. 4, large variations in the shear and expansion parameters give only small changes in the lattice constants. With different values of σ_{1x}, σ_{1y}, ε_1 and σ_{2x}, σ_{2y}, ε_2 their effect upon the differences between the lattice parameters for the two lamellae was examined. The maximum possible variations in the parameters σ_{ix}, σ_{iy} and ε_i $(i=1,2)$ within the experimental accuracy involve small changes $\delta(\Delta q)$ in the difference Δq between the lattice parameters q_1 and q_2. q_i $(i=1,2)$ denotes one of the six lattice parameters

Table 2. *Lattice parameters of labradorite feldspars*

Specimen	Phase	*a* (Å)	*b* (Å)	*c* (Å)	α (°)	β (°)	γ (°)	*V* (Å³)
L	Mean (X-ray)	8·178 (1)	12·865 (1)	7·115 (1)	93·55 (1)	116·23 (1)	89·76 (1)	670·0
	Phase 1	8·181 (1)	12·862 (4)	7·115 (1)	93·57 (2)	116·24 (1)	89·84 (2)	
	Phase 2	8·175 (1)	12·868 (4)	7·115 (1)	93·53 (2)	116·22 (1)	89·68 (2)	
A	Mean (X-ray)	8·178 (2)	12·871 (4)	7·113 (2)	93·58 (4)	116·25 (2)	89·71 (4)	670·0
	Phase 1	8·181 (2)	12·868 (4)	7·112 (2)	93·60 (4)	116·26 (2)	89·80 (4)	
	Phase 2	8·176 (2)	12·871 (4)	7·114 (2)	93·53 (4)	116·25 (2)	89·65 (4)	
*A*1	Mean (X-ray)	8·177 (2)	12·877 (4)	7·117 (2)	93·54 (3)	116·24 (2)	89·64 (3)	670·7

Specimen	Phase	a^* (Å^{-1})	b^* (Å^{-1})	c^* (Å^{-1})	α^* (°)	β^* (°)	γ^* (°)
L	Mean (X-ray)	0·13636	0·07791	0·15703	86·16	63·73	88·52
	Phase 1	0·13633	0·07793	0·15706	86·10	63·72	88·42
	Phase 2	0·13639	0·07788	0·15701	86·22	63·75	88·62
A	Mean (X-ray)	0·13638	0·07787	0·15711	86·15	63·71	88·56
	Phase 1	0·13635	0·07789	0·15716	86·08	63·70	88·44
	Phase 2	0·13641	0·07786	0·15707	86·24	63·72	88·65
*A*1	Mean (X-ray)	0·13638	0·07783	0·15699	86·23	63·73	88·65

for lamella No. i. The maximum variation in Δq due to allowed variations in σ_{ix}, σ_{iy}, ε_i ($i=1,2$) is given in Table 3. Two points should be noted: (1) the parameters σ_{iy} have small influence upon the accuracy; (2) the b axis is difficult to determine since this axis is nearly normal to the boundary between the lamellae.

The splitting of the Kikuchi lines is a measure of the difference $\Delta q=q_1-q_2$ between the lattice parameters of the two lamellae, whereas the X-ray diffraction measurements determine $q=v_1q_1+v_2q_2$ where v_1 and v_2 are the volume fractions of the lamellae 1 and 2. Since v_1 and v_2 are approximately equal to $\frac{1}{2}$, it is assumed in the following discussion that $q=\frac{1}{2}(q_1+q_2)$. Hence the following relations between the uncertainties $s_{\Delta q}$, s_{qi} and s_q in the parameters Δq, q_i and q hold:

$$\text{(1) from Kikuchi lines: } s_{qi}=\frac{1}{\sqrt{2}}s_{\Delta q},$$

$$\text{(2) from X-ray diffraction: } s_{qi}=s_q. \qquad (13)$$

From these relations the accuracy of the lattice parameters can be determined. The uncertainties in the differences ($s_{\Delta q}$) and in the mean lattice constants (s_q) found from the X-ray diffraction are shown in Tables 4 and 2. From the relations (13) the contributions to the uncertainties in the different lattice parameters from the split Kikuchi lines and the X-ray diffraction may be compared. A main conclusion is that the uncertainties in the lattice parameters are determined mainly by the uncertainties in the X-ray measurements except for the b axes, where it is determined by the split-Kikuchi-line measurements. The accuracy of the different lattice constants is given in Table 2.

Table 4. *The uncertainties in the difference between the lattice parameters of the two lamellae*

Specimen	$s_{\Delta a}$(Å)	$s_{\Delta b}$(Å)	$s_{\Delta c}$(Å)	$s_{\Delta\alpha}$(°)	$s_{\Delta\beta}$(°)	$s_{\Delta\gamma}$(°)
L	0·001	0·006	0·001	0·03	0·01	0·03
A	0·001	0·006	0·001	0·03	0·01	0·03

Since the split-Kikuchi-line method is based on assumption of invariant boundaries, the influence of the orientation of the boundaries on the accuracy of the lattice parameters was investigated. It was found that an error in the orientation of about 8–9° gave variations in the lattice parameters less than the accuracy shown in Table 2. Some examples are shown in Fig. 5 for specimen L.

The lattice constants

The above analysis leads to the result that a significant difference exists between the a axes and the angles γ in the two labradorite lamellae. The difference in the a axes can easily be explained by the charac-

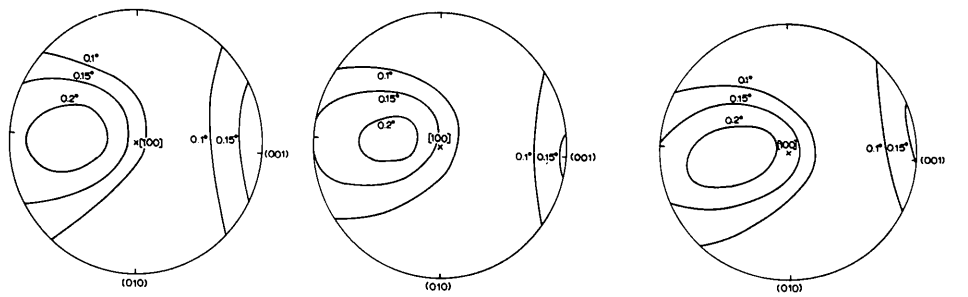

Fig. 4. Examples of the effect of the variations in the shear and expansion parameters upon the theoretical φ values for specimen A. σ_{1x}, σ_{2y} and ε_1 in respectively (*a*), (*b*) and (*c*) are different from the values given in Fig. 3(*b*).

Table 3. *The maximum variation in the difference between the lattice parameters of the two lamellae due to allowed variations in σ_{ix}, σ_{iy} and ε_i*

Specimen	Parameter	$\delta(\Delta a)$ (Å)	$\delta(\Delta b)$ (Å)	$\delta(\Delta c)$ (Å)	$\delta(\Delta\alpha)$ (°)	$\delta(\Delta\beta)$ (°)	$\delta(\Delta\gamma)$ (°)
L	σ_{ix}	0·001	0·003	0·001	0·03	0·01	0·03
	σ_{iy}	–	–	0·001	–	–	0·01
	ε_i	0·001	0·006	–	0·02	–	0·02
A	σ_{ix}	0·001	0·003	–	0·03	0·01	0·03
	σ_{iy}	–	–	–	–	–	–
	ε_i	0·001	0·006	0·001	0·02	–	0·01

teristic double-crankshaft in the feldspar structure. This crankshaft consists of four-membered rings, alternately horizontal and vertical, extending along the *a* axis and can expand or contract in response to substitution of *M* cations, to thermal vibrations and to stress between different domains. For alkali feldspars many specimens have anomalous *a* axis dimensions because during segregation of Na and K in perthites, the aluminosilicate framework may retain complete or partial continuity with consequent distortion of the cell dimensions of the two components (Stewart & Wright, 1974). Similar behaviour may be expected for plagioclases.

From X-ray microanalysis of the composition of the two labradorite lamellae (Olsen, 1976*b*; Olsen & Lillebö, 1976), it has been found that the An content varies from about 40 to 60 mol % in these specimens. Previous X-ray diffraction studies of the variation of the cell dimensions with mol % An have shown that only small changes in the lattice constants may be expected in this composition range, except for the angle γ (Bambauer, Eberhard & Viswanathan, 1967). This is consistent with the present findings.

Cell dimensions of feldspars depend on three main factors: the chemical composition, the ordering of the atoms and the degree of coherence between domains in the crystal. For alkali feldspars it has been shown that measurements of lattice parameters can give information about these three factors. For plagioclases, however, the cell dimensions correlate so closely with each other that separate determination of the An content and the structural state has previously been impossible or unreliable for most plagioclases. Although the An content in the lamellae has been determined separately by X-ray microanalysis, dark-field microscopy revealed very complicated domain structures in the investigated specimens which make it difficult to reach any conclusion about the structural state on the basis of the lattice parameters.

One of the investigated specimens *A*1 showed no exsolution. The lattice constants for this specimen obtained from X-ray diffraction are in very good agreement with the results for phase 2 in the specimens *L* and *A* as determined by the split-Kikuchi-line method.

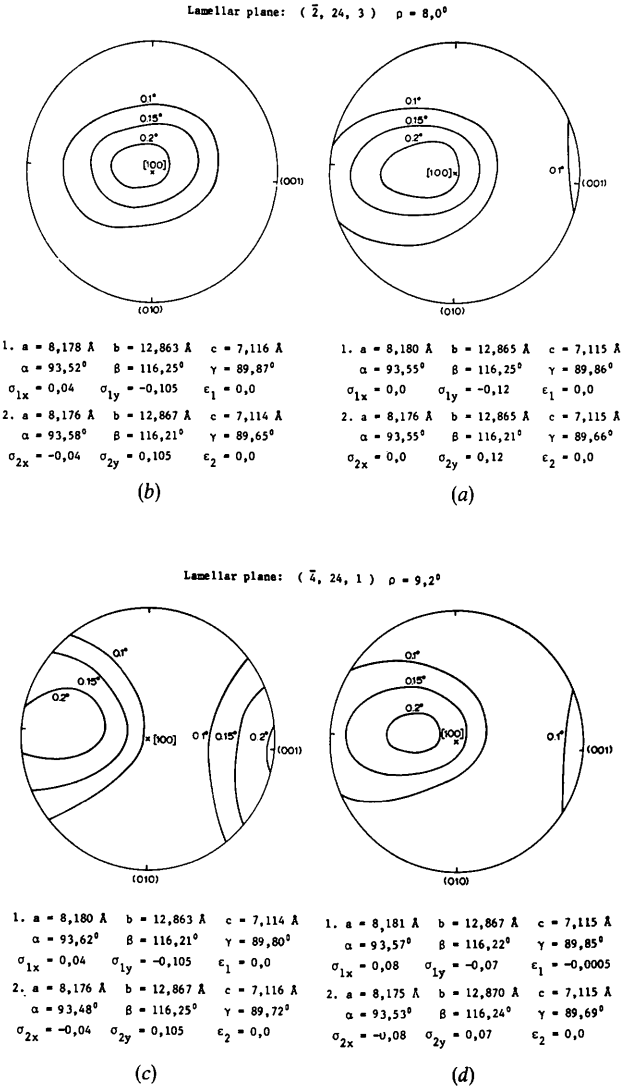

Fig. 5. Examples showing the influence of the orientation of the boundaries upon the accuracy of the lattice parameters. In (*a*) and (*c*) the same shear and expansion parameters have been used as given in Fig. 3(*a*) whereas in (*b*) and (*d*) these parameters are changed in order to get a better fit with the curves in Fig. 3(*a*). ρ is the angle between the lamellar plane and ($\bar{4}$,24,3). Specimen: *L*.

Conclusion

The split Kikuchi line method has proved very useful for determining lattice parameters of slightly different lamellar structures. The uncertainties in the parameters are mainly determined by the uncertainties in the X-ray measurements except for the axes normal to the boundary between the lamellae where they are inherent in the split-Kikuchi-line measurements.

In the present investigation significant differences could be measured between the lattice parameters *a* and between the angles γ for the two lamellae. The magnitudes of these differences are about 0·005 Å and 0·15° respectively.

Although there is good agreement between the lattice parameters obtained from the different specimens, the present study is based only on three samples. Since the variations in the cell dimensions in the composition range from 40 to 60 mol % An are so small, more crystals need to be examined before a complete understanding of the variations in the lattice parameters is obtained.

The author wishes to thank Dr W. L. Griffin for performing the electron microprobe analyses and Dr

J. Gjönnes for his interest in the present work. The labradorite specimens came from the collection of the Mineralogical–Geological Museum, Oslo.

APPENDIX

$$S_{11}=b^2c^2\sin^2\alpha,$$
$$S_{22}=c^2a^2\sin^2\beta,$$
$$S_{33}=a^2b^2\sin^2\gamma,$$
$$S_{12}=abc^2(\cos\alpha\cos\beta-\cos\gamma),$$
$$S_{23}=a^2bc(\cos\beta\cos\gamma-\cos\alpha),$$
$$S_{13}=ab^2c(\cos\gamma\cos\alpha-\cos\beta),$$
$$V^2=a^2b^2c^2(1-\cos^2\alpha-\cos^2\beta-\cos^2\gamma+2\cos\alpha\cos\beta\cos\gamma),$$
$$M^2=\frac{1}{d_{pqr}^2}=\frac{1}{V^2}(S_{11}p^2+S_{22}q^2+S_{33}r^2+2S_{12}pq+2S_{23}qr+2S_{31}pr).$$

References

BAMBAUER, H. U., EBERHARD, E. & VISWANATHAN, K. (1967). *Schweiz. Miner. Petrogr. Mitt.* **47**, 351–364.

BOLLMANN, W. (1970). *Crystal Defects and Crystalline Interfaces*. Berlin: Springer.

BOWN, M. G. & GAY, P. (1958). *Z. Kristallogr.* **111**, 1–14.

CLIFF, G., CHAMPNESS, P. E., NISSEN, H.-U. & LORIMER, G. W. (1976). *Electron Microscopy in Mineralogy*, pp. 258–265. Berlin: Springer.

FAIVRE, P. (1975). *J. Appl. Cryst.* **8**, 356–360.

HASHIMOTO, H., KUMAO, A., ENDOH, H., NISSEN, H.-U., ONO, A. & WATANABE, E. (1976). *Developments in Electron Microscopy and Analysis*, pp. 245–250. New York: Academic Press.

HASHIMOTO, H., NISSEN, H.-U., ONO, A., KUMAO, A., ENDOH, H. & WOENSDREGT, C. F. (1976). *Electron Microscopy in Mineralogy*, pp. 332–344. Berlin: Springer.

HIRSCH, P. B., HOWIE, A., NICHOLSON, R. B., PASHLEY, D. W. & WHELAN, M. J. (1965). *Electron Microscopy of Thin Crystals*. London: Butterworths.

HØIER, R. (1969). *Acta Cryst.* A**25**, 516–518.

JOHARI, O. & THOMAS, G. (1969). *The Stereographic Projection and its Applications, Techniques of Metals Research*. Vol. II*a*. New York: Interscience.

MCLAREN, A. C. & MARSHALL, D. B. (1974). *Contr. Miner. Petrol.* **44**, 237–249.

NISSEN, H.-U. & BOLLMANN, W. (1968). *Proc. 4th Eur. Reg. Conf. Electron Microscopy, Rome*, pp. 321–322.

NISSEN, H.-U., CHAMPNESS, P. E., CLIFF, G. & LORIMER, G. W. (1973). *Nature, Lond.* **245**, 135–137.

OLSEN, A. (1976*a*). *J. Appl. Cryst.* **9**, 9–13.

OLSEN, A. (1976*b*). *Proc. 6th Eur. Conf. Electron Microscopy, Jerusalem*, Vol. 1, pp. 417–418.

OLSEN, A. & LILLEBÖ, V. (1976). *Developments in Electron Microscopy and Analysis*, pp. 489–492. New York: Academic Press.

PIROUZ, P. & BOSWARVA, I. M. (1974). *Phys. Stat. Sol.* (*a*), **26**, 407–415.

PUMPHREY, P. H. & BOWKETT, K. M. (1970). *Phys. Stat. Sol.* (*a*), **2**, 339–346.

SMITH, J. V. (1974*a*). *Feldspar Minerals*, Vol. I. New York: Springer.

SMITH, J. V. (1974*b*). *Feldspar Minerals*, Vol. II. New York: Springer.

STEWART, D. B. & WRIGHT, T. L. (1974). *Bull. Soc. Fr. Minér. Crist.* **97**, 356–377.

Acta Cryst. (1977). A**33**, 712–716

Solving Structures with Quartets: The Least-Squares Analysis of Quartet Invariants in Space Group *P*1

BY CHRISTOPHER J. GILMORE

Department of Chemistry, University of Glasgow, Glasgow G12 8QQ, Scotland

(*Received* 26 *March* 1977; *accepted* 29 *April* 1977)

A least-squares technique for extracting individual phase angles from a set of quartet invariants is described. For symmorphic space groups, this procedure offers the advantages of stability and, in non-centrosymmetric cases, a systematic way of defining the enantiomorph, in contrast with traditional direct methods employing triplets. The application to a phthalic anhydride derivative $C_{26}H_{16}O_5$ in space group *P*1 is described. The method is readily extended to other space groups.

1. Introduction

Crystal structures in space group *P*1 are traditionally the most difficult to solve by direct methods. The symmorphic nature of the space group tends to make the process ill-conditioned, and the lack of equivalent reflexions gives rise to a paucity of sign relations of low associated variance. This forces the need for a relatively large starting set which, in turn, implies a large number of possible solutions from which the correct phase set may be difficult to extract. Enantiomorph definition is often a haphazard affair, since it is difficult to predict accurately those invariants with magnitudes sufficiently far from 0 or π.